2276 *Biochemistry* **1995,** *34,* 2276−2283

Stringent and Relaxed Specificities of *Taq*I Endonuclease: Interactions with Metal Cofactors and DNA Sequences[†]

Weiguo Cao, Alan N. Mayer, and Francis Barany*

Department of Microbiology, Hearst Microbiology Research Center, Cornell University Medical College,
1300 York Avenue, Box 62, New York, New York 10021

Received October 4, 1994; Revised Manuscript Received December 1, 1994[⊗]

ABSTRACT: We have studied the roles of metal cofactors Mg^{2+} and Mn^{2+} in modulating substrate specificities during the enzymatic cycle of *Taq*I endonuclease using steady state and single-turnover kinetics. In the presence of Mg^{2+}, stringent discrimination of *Taq*I against single base-pair changes (star sites) is manifested by the loss of tight, specific binding in the early stage of the enzymatic cycle. In the presence of Mn^{2+}, relaxed specificity for a star site sequence is attributed to formation of three distinct classes of the ternary complexes: the highly activated *Taq*I−cognate−Mn^{2+} complex; the partially activated *Taq*I−star−Mn^{2+} complex; and the ground state, inactive *Taq*I−nonspecific−Mn^{2+} complex. In addition to a high affinity for a *Taq*I−DNA complex, Mn^{2+} also binds to *Taq*I in a DNA-independent fashion. This may facilitate enzyme activation, which could account for the observed relaxation in substrate specificity. Thus, the *Taq*I−DNA−Mn^{2+} complex could be formed by either of two pathways: *Taq*I binding to DNA followed by the binding of Mn^{2+} or *Taq*I first binding to Mn^{2+} followed by the addition of DNA. The inactive, nonspecific *Taq*I−star−Mg^{2+} complex virtually prohibits transition state interactions, but a *Taq*I−star−Mn^{2+} complex attains a measurable single-turnover rate. In the late stages of the enzymatic cycle, high affinity of Mn^{2+} to a *Taq*I−DNA complex and to the *Taq*I enzyme may also account for a slower rate of product release.

The specificity of restriction endonucleases relies on the interactions among the enzyme, DNA, and metal cofactors (Smith, 1979; Aiken et al., 1991; Rosenberg, 1991; Heitman, 1993; Roberts & Halford, 1993). Much of our knowledge about restriction enzymes is based on studies of *Eco*RI and *Eco*RV endonucleases, for which different mechanisms of molecular recognition have been proposed (Lesser et al., 1990; Halford et al., 1993). While the *Eco*RI endonuclease demonstrates specific binding to its cognate sequence in the absence of metal cofactor, *Eco*RV endonuclease makes specific contacts with its cognate site only in the presence of metal cofactor. The energetics of *Eco*RI−DNA interactions have been rigorously probed by systematically altering the recognition site using base analogues and single base-pair substitutions (Lesser et al., 1990, 1993). The specificity of *Eco*RI recognition is achieved at several levels, including DNA binding, distortion, and transition state interactions. The relative activity of *Eco*RV toward cognate versus noncognate DNA seems to stem from an altered affinity of metal cofactors for the enzyme−DNA complex (Taylor & Halford, 1989, 1992; Taylor et al., 1990, 1991; Vermote & Halford, 1992; Vermote et al., 1992).

*Taq*I restriction endonuclease hydrolyzes the phosphodiester bond between the T and C of the recognition sequence TCGA (Barany, 1988b; Zebala et al., 1992a,b). Kinetic analysis has shown that both high temperature and Mg^{2+} are required for specific binding and catalysis (Zebala et al., 1992a). Previous studies designed to probe the *Taq*I−DNA interactions evaluated cleavage of star sites using Mg^{2+} as the cofactor in the presence of dimethyl sulfoxide (DMSO) (Barany, 1988a). On the basis of the relative cleavage rates of star sites, an eight-hydrogen bond (direct readout) model was proposed, in which it was suggested that N^4 of C, N^7 of G, and N^6 and N^7 of A acted as hydrogen bond donors or acceptors. This model was then superseded by the results of a base analogue study, in which the proposed major groove contacts were isosterically substituted and then subjected to kinetic analysis (Zebala et al., 1992b). Base analogue substitutions within the cognate site revealed that N^6 (the *in vivo* methylation site) and N^7 of A and N^7 of G form specific enzyme−DNA contacts during the transition state. In addition, the role of the phosphate backbone was investigated using ethylation interference of cleavage (Zebala et al., 1992b). Under standard conditions, the phosphates **TpCpG-pAp** were required for cleavage of the modified strand. Under star conditions, ethylation of the phosphate 3′ to the A did not abolish enzymatic activity. The effects of sulfur substitutions for the nonbridging *pro*-R_p oxygens were mostly confined to the scissile phosphate position. The phosphate contacts were further pinpointed by evaluating the roles of individual phosphates in both binding and catalysis using S-methylated substrates (Mayer & Barany, 1994). This study indicated that primary phosphate contacts are established during binding at **pTpCp**GpAp positions (shown in bold). Transition state stabilization requires additional contacts at pTpCpG**pAp** positions; in particular, the G**p**A contact may serve as a controlling point to mediate the transformation from the ES state to the transition state.

[†] W.C. is a Norman and Rosita Winston Foundation Fellow in Biomedical Research. F.B. is supported in part by a Hirschl/Monique Weill-Caulier Career Scientist Award. This work was supported by grants from the National Institutes of Health (GM-41337-05) and the Applied Biosystems Division of the Perkin Elmer Corp.

* Corresponding author. Tel.: 212-746-6507. Fax: 212-746-8587. email: barany@cumc.cornell.edu.

[⊗] Abstract published in *Advance ACS Abstracts,* February 1, 1995.

0006-2960/95/0434-2276$09.00/0

The protein–DNA contacts revealed in previous studies do not fully account for the several millionfold specificity of *Taq*I. The present work addresses this problem by examining other possible sources of specificity, such as the interrelationships among the enzyme, metal cofactor, and cognate, star site, and nonspecific DNA. To identify the steps in the catalytic cycle during which these interactions are relevant, both steady state and single-turnover kinetic analyses were performed. The data reveal that sequence discrimination by *Taq*I is mediated by the metal cofactor during ES binding in the early enzymatic cycle. The higher affinity of Mn^{2+} for the *Taq*I–DNA complex correlates with lowered sequence selectivity, thus supporting the notion that the ternary complex binding energy may underlie sequence discrimination. This study reports direct interactions between Mn^{2+} and *Taq*I in the absence of DNA. This may result in formation of a complex which is energetically closer to the transition state and thus is more tolerant of single base-pair changes. In the case of Mg^{2+}, a single base-pair change may interfere with ternary complex formation, precluding cleavage of noncognate DNA.

EXPERIMENTAL PROCEDURES

Materials. *Taq*I endonuclease was purified as previously described (Barany, 1988b). Sequenase 2.0 was from U.S. Biochemicals (Cleveland, OH). T4 polynucleotide kinase was from New England Biolabs (Beverly, MA). Bacterial alkaline phosphatase from Pharmacia (Piscataway, NJ) was obtained as a suspension (in 40% ammonium sulfate) and centrifuged. The pellet was dissolved in 100 mM Tris-HCl buffer (pH 8.0) containing 10 mM $ZnCl_2$ to a final concentration of 10 units/mL prior to storage at 4 °C. Kinase-ligase buffer (kin-lig buffer) consisted of 50 mM Tris-HCl, pH 8.0, 10 mM $MgCl_2$, 1 mM EDTA, and 6 mM β-mercaptoethanol. Oligonucleotides were synthesized using an Applied Biosystems 381 DNA synthesizer. Nonmodified oligonucleotides were purified on denaturing sequencing gel (7 M urea/10% polyacrylamide) (Applied Biosystems Inc., 1992). Hairpin oligonucleotide (see Steady State Experiments) was purified on 40% formamide denaturing gel (United States Biochemical, 1992). Manganese solutions were acidified by addition of HCl (1 mM) and stored at −20 °C prior to use (Smith et al., 1992). Nucleotide triphosphates were purchased from Sigma Chemicals (St. Louis, MO).

Single-Turnover Experiments. Star site oligonucleotides were created for kinetic analysis by changing one base pair at a time within the cognate site of the following oligonucleotides:

5′-ACT CAC CAA TCG ATT TAC CGG GTG GCA GCC TGG CAT GCC T-3′

3′-TGA GTG GTT AGC TAA ATG GCC CAC CGT CGG ACC GTA-5′

A total of six star site oligonucleotides were synthesized (Table 2). For 5′-end labeling, typically 20 pmol of each oligonucleotide was labeled with [γ-^{32}P]ATP (20 pmol, 6000 Ci/mmol; Du Pont-NEN, Wilmington, DE) in kin-lig buffer (20 μL) containing dithiothreitol (10 mM) and T4 polynucleotide kinase (10 units). The reaction mixture was incubated at 37 °C for 1 h, and then kinase was inactivated at 65 °C for 10 min. After the addition of 2 μL of 0.5 M EDTA and 2 μL of loading buffer (0.1% bromophenol blue, 0.1% xylene cyanol, 50% glycerol, 50 mM EDTA), oligonucleotides were separated from [γ-^{32}P]ATP by gel filtration chromatography on Sephadex G-25 columns containing 10 mM ammonium acetate, pH 8.0. They were then adjusted to equal radiospecificity (4 × 10^6 cpm/pmol) by the addition of unlabeled oligonucleotides. Equimolar amounts of top strand and bottom strand oligonucleotides were mixed and heated at 85 °C for 10 min and then cooled slowly at room temperature to allow the formation of duplex oligonucleotide, which was verified by nondenaturing polyacrylamide gel electrophoresis. Single-turnover experiments were performed at 60 °C in the presence of 2 mM Mn^{2+} or 10 mM Mg^{2+}. The prereaction mixture contained 0.25 μL of 0.1 μM duplex DNA (0.025 pmol), 2.5 μL of 2 μM *Taq*I endonuclease (200-fold in excess of DNA concentration, which ensured complete saturation of oligonucleotide substrate; data not shown), 1 μL of 100 mM Tris-HCl (pH 8.0 at 60 °C), 1 μL of 1 mg/mL bovine serum albumin (BSA), 0.5 μL of 200 mM dithiothreitol, and 3.75 μL of deionized water. [Low-salt buffer was used to enhance star activity (Polisky et al., 1975; Halford et al., 1986; Taylor & Halford, 1989)]. This mixture was equilibrated for 3–5 min at 60 °C, and then the reaction was initiated by adding 9 μL of the prereaction mixture to 1 μL of 20 mM $MnCl_2$ or 1 μL of 100 mM $MgCl_2$. At each time point, a 9 μL aliquot of the reaction mixture was removed and added to 10 μL of stop buffer (95% formamide, 20 mM EDTA, 0.05% bromophenol blue, and 0.05% xylene cyanol) to quench the reaction. After electrophoresis on 10% denaturing sequencing gel, cleavage products and unused substrates were quantified using a PhosphorImage (Molecular Dynamics, Sunnyvale, CA). Rate constants were obtained by nonlinear curve fitting (Figure 1) using the computer program MINSQUARE (MicroMath, Salt Lake City, UT). The free energy change was calculated using eq 1 (Lesser et al., 1990).

$$\Delta\Delta G^{\ddagger} = -RT \ln(k_{st}/K_d \text{ modified}/k_{st}/K_d \text{ unmodified}) \qquad (1)$$

Steady State Experiments. A 42-mer hairpin oligonucleotide was synthesized and then purified on a 40% formamide gel. The hairpin oligonucleotide (100 pmol) was extended in 1× Sequenase buffer (40 μL; U.S. Biochemical) containing 1.7 μM [α-^{32}P]dCTP (6000 Ci/mol), 125 μM triphosphate nucleotide mix (dATP, dGTP, dTTP), 5 mM dithiothreitol, and 5 units of Sequenase 2.0 (U. S. Biochemical) for 1 h at 37 °C. The product was purified by gel filtration chromatography on the Sephadex G-25 column as described previously (Zebala et al., 1992a). The purified oligonucleotide was lyophilized and dissolved in TE (10 mM Tris, 1 mM EDTA, pH 8.0) to a final concentration of 0.1 μM. The complete reaction mixture (500 μL) consisted of 0.1 mg/mL BSA, 10 mM dithiothreitol, 10 mM Tris-HCl (pH 8.0 at 60 °C), *Taq*I endonuclease, substrate (hairpin oligonucleotide), and the metal cofactors. Enzyme–substrate ratio was 100:1 for Mg^{2+} and 25:1 for Mn^{2+}. The substrate concentrations ranged from 0.25, 0.5, 1, 2, and 4 to 8 nM. The prereaction mixture (450 μL) contained no metal cofactor and was preincubated at 60 °C for 3–5 min, and the reaction was initiated by adding 50 μL of 100 mM $MgCl_2$ or 50 μL of 20 mM $MnCl_2$ to the prereaction mixture. At each time point, 100 μL of reaction mixture was withdrawn and added to 10 μL of 150 mM EDTA. After *Taq*I endonuclease was inactivated at 85 °C for 15 min, 25 μL of BAP solution (0.006 unit/mL bacterial alkaline phosphatase, 30 mM Tris-HCl, pH 8.0 at 60 °C, 40 mM $MgCl_2$) was added and the reaction mixture incubated at 65 °C for 15 min. This allowed the exposed ^{32}P from *Taq*I endonuclease cleavage to be completely hydrolyzed by phosphatase (Zebala et al., 1992a). Oligonucleotides were precipitated by addition of sonicated salmon sperm DNA (20 μL of 10 mg/mL) and trichloroacetic acid (20 μL of 50%). The radioactivity in both supernatant and pellet was measured by Cerenkov counting. Cleavage was represented by $\mathrm{cpm}_{(\mathrm{supernatant})}/[\mathrm{cpm}_{(\mathrm{supernatant})} + \mathrm{cpm}_{(\mathrm{pellet})}]$. Steady state constants were obtained by fitting data into the Michaelis–Menten equation using the computer program ULTRAFIT (Biosoft, Ferguson, MO).

For measurement of dissociation constants, oligonucleotides containing an N^7-deaza-A substitution, a phosphorothioate at the scissile phosphate, or star sites (competitor) were used in competition experiments. The competitor concentrations varied by 0.5, 1, 2, and 3 times its K_i value. To insure that the substrate concentration was varied across the apparent K_m, the substrate (hairpin oligonucleotide) concentrations for each competitor concentration were adjusted by the following relationship:

$$[S]_i = 1 + [S]/K_i \qquad (2)$$

where [S] is the substrate concentration without competitor (Segel, 1975). The enzyme–substrate ratio was kept at 1:100 for Mg^{2+} and at 1:25 for Mn^{2+}. K_i values were obtained by primary plots of cleavage versus time, by reciprocal plots of rates versus substrate concentrations, and then by secondary plots of apparent K_m versus competitor concentrations (Segel, 1975) using the computer program Cricket Graph (Computer Associate, Garden City, NY).

Metal Interaction with TaqI–DNA Complexes. Experiments were performed under single-turnover conditions. Mg^{2+} and Mn^{2+} concentrations were varied in the range of 0.5–20 mM and 0.1–5 mM, respectively. Incubation time was adjusted wherever possible to obtain 10–90% cleavage. The reaction mechanism was described as follows:

$$\mathrm{ES} + \mathrm{M}^{2+} \overset{K_d}{\rightleftharpoons} \mathrm{ESM}^{2+} \xrightarrow{k_2} \mathrm{EPM}^{2+} \qquad \text{(Scheme 1)}$$

$$V = k_2[\mathrm{ESM}^{2+}] \qquad (3)$$

$$K_d = \frac{[\mathrm{ES}][\mathrm{M}^{2+}]}{[\mathrm{ESM}^{2+}]} \qquad (4)$$

$$V = \frac{k_2[\mathrm{ES}]_T[\mathrm{M}^{2+}]}{K_d + [\mathrm{M}^{2+}]} \qquad (5)$$

RESULTS

Rate of Single-Turnover Cleavage with Mg^{2+} or Mn^{2+}. Restriction enzymes typically have single-turnover rate constant (k_{st}) values in the range of 3–15 min^{-1}, which makes it possible to measure this constant without the use of a stopped-flow apparatus. We designed the double stranded oligonucleotides with the target site embedded in an AT rich environment (Figure 1A). The six star sites were created by systematically changing one base pair within the cognate sequence so that the substitutions occurred within a constant local environment. After electrophoresis on 10% polyacrylamide denaturing sequencing gels, the radiolabeled products and substrates (40-mer for top strand, 36-mer for bottom strand) were quantified using a PhosphorImager. As shown in Figure 1A, cleavage of both strands produced two 5′-end-labeled products, a 10-mer from the top strand and a 24-mer from the bottom strand. The cleavage reaction can be described by two linked mathematical equations (Figure 1B), in which k_2 and k_3 represent the first nicking events of the top and bottom strands, respectively. k_4 and k_5 describe the cleavage of the nicked intermediate (Fersht, 1985; Lesser et al., 1990), assuming the enzyme remained bound to

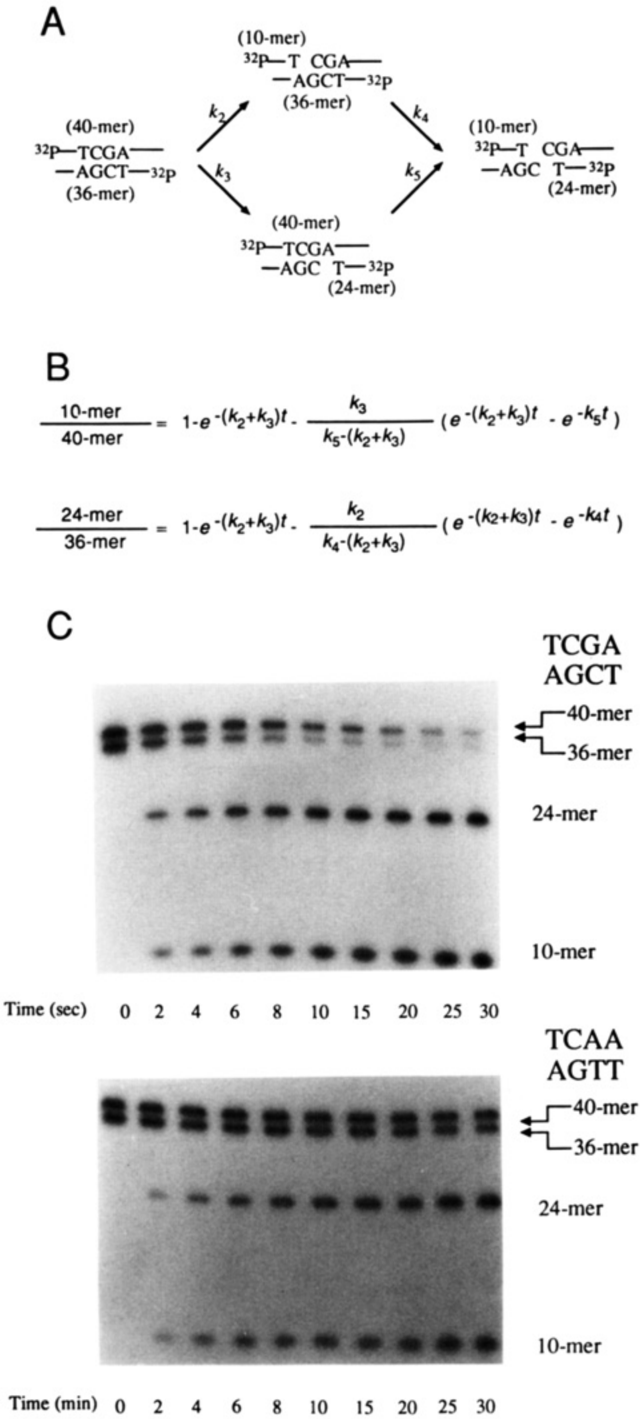

$$\frac{\text{10-mer}}{\text{40-mer}} = 1 - e^{-(k_2+k_3)t} - \frac{k_3}{k_5-(k_2+k_3)}\left(e^{-(k_2+k_3)t} - e^{-k_5 t}\right)$$

$$\frac{\text{24-mer}}{\text{36-mer}} = 1 - e^{-(k_2+k_3)t} - \frac{k_2}{k_4-(k_2+k_3)}\left(e^{-(k_2+k_3)t} - e^{-k_4 t}\right)$$

FIGURE 1: Kinetic analysis strategy. A. Cleavage pattern. B. Mathematical expression of double- strand cleavage. C. Experimental data. Top diagram shows cleavage of canonical site of *Taq*I endonuclease in the presence of 2 mM MnCl$_2$ under single-turnover conditions (from left to right: 0, 2, 4, 6, 8, 10, 15, 20, 25, and 30 s). Bottom diagram shows cleavage of preferred star site (TCAA/AGTT) under the same conditions (from left to right: 0, 2, 4, 6, 8, 10, 15, 20, 25, and 30 min). Products were separated on 10% denaturing sequencing gels. Intensity of bands was quantified on a PhosphorImager. Experimental data were fitted into these models simultaneously using the nonlinear curve-fitting program, MINSQUARE.

Table 1: Single-Turnover Rate Constants in the Presence of Mg^{2+}[a]

Site	k_2 (min^{-1})	k_3 (min^{-1})	k_4 (min^{-1})	k_5 (min^{-1})
TCGA	2.8 (±0.72)		0.9 (±0.27)	
AGCT		2.7 (±0.7)		0.6 (±0.17)
TsCG A[b]	0.20 (±0.02)		0.17 (±0.03)	
A GCsT		0.28 (±0.01)		0.1 (±0.014)
TCG^{7c}A[c]	0.31 (±0.05)		0.15 (±0.008)	
^{7c}AGC T		0.32 (±0.015)		0.1 (±0.02)
star sites	negligible	negligible	negligible	negligible

[a−c] See footnotes for Table 2.

substrate. The ratios of product to total substrate were determined by quantifying intensities of the corresponding bands (Figure 1C). Rate constants were obtained by fitting experimental data into these equations simultaneously using the computer program MINSQUARE.

With Mg^{2+} as the cofactor, nicking of the top and bottom strands occurred at very similar rates (Table 1). The values of 2.8 and 2.7 min^{-1} were lower than the previously reported k_{st} rate constants (Zebala et al., 1992a), possibly due to the use of a low-salt buffer in our experiments. Under these conditions, the rate of the second nicking event was 3−5 times lower than those of the first nicking event. Previous data using a plasmid substrate suggested that both first and second nicking events occur at similar rates (Zebala et al., 1992a); the present results may be a consequence of the oligonucleotide substrate. The single-turnover rates of the first nicking events with phosphorothioate at the scissile phosphate position or with the N^7-deaza-A substitution were about 10-fold lower than those for the unmodified cognate sequence (Table 1). Single base-pair substitutions resulted in negligible cleavage using Mg^{2+} as the cofactor (Table 1).

With Mn^{2+} as the cofactor, the single-turnover rates of both nicking events for the cognate site were greater than those with Mg^{2+} (Table 2). In addition, Mn^{2+} elicited a latent strand preference not seen with Mg^{2+}, the bottom strand being reproducibly cleaved twice as fast as the top strand. The rate of the first nicking event for the top strand was increased by about 3-fold, while the bottom strand was increased by about 5-fold relative to that with Mg^{2+}. This difference in cleavage rates may stem from flanking sequence effects (W. Cao and F. Barany, unpublished data). As with Mg^{2+}, the rates of the second nicking event were severalfold lower than those of the first nicking event.

The enzyme exhibited a higher tolerance to base and phosphate analogue substitutions using Mn^{2+} as the cofactor, as modifications lowered the single-turnover rates one-half as much for Mn^{2+} as compared to Mg^{2+}. In the presence of Mn^{2+}, rates of the first nicking events for the R_P-phosphorothioate and N^7-deaza-A-substituted oligonucleotides were lowered 5-fold relative to the unsubstituted sequence (Table 2). Mn^{2+} lowered the stringency of discrimination against star sites as well. One of the six star sites (TC$\underline{\text{A}}$A/AG$\underline{\text{T}}$T) exhibited a cleavage rate considerably greater than the others (Table 2). For this "preferred" star site, the rate constants for the first nicking event of both strands were similar. For the other five star sites, the rate constants for the first nicking event showed a 10−20-fold strand preference (Table 2). The data are qualitatively similar to the previous analysis of the star reaction using DMSO and Mg^{2+} (Barany, 1988a) and may result from the combined effects of contact loss and the introduction of asymmetry into the enzyme−DNA complexes. As with *Eco*RI, single base-pair changes may produce asymmetrical structural adaptations (Lesser et al., 1990).

Interactions between TaqI and DNA Sequences. A base modification or a base substitution in the cognate sequence may affect catalysis, *Taq*I−DNA binding, or both. Since K_m is a composite constant, it may not reveal genuine changes in substrate binding by an enzyme, especially when a nonchemical step is rate limiting (Lesser et al., 1990; Fersht, 1985). To determine the effects of single base-pair changes on the binding constant, we used analogue-substituted cognate sequences or star site sequences as competitive inhibitors in a steady state assay. Since these oligonucleotides are cleaved much more slowly than the cognate sequence, it was possible to accurately measure the K_i of these oligonucleotides under steady state conditions. Double-reciprocal plots of these data confirm that these oligonucleotides act as competitive inhibitors of *Taq*I endonuclease (Figure 2). Thus, for the measured inhibition constants,

Table 2: Single-Turnover Rate Constants in the Presence of Mn^{2+}[a]

site	k_2 (min^{-1})	k_3 (min^{-1})	k_4 (min^{-1})	k_5 (min^{-1})
TCGA	7.4 (±1.02)		4.3 (±0.42)	
AGCT		13.2 (±2.05)		3.4 (±0.26)
TsCG A[b]	1.0 (±0.04)		0.71 (±0.32)	
A GCsT		2.5 (±0.17)		1.0 (±0.04)
TCG^{7c}A[c]	1.75 (±0.48)		0.75 (±0.04)	
^{7c}AGC T		2.29 (±0.53)		0.27 (±0.04)
$\underline{\text{C}}$CGA	1.8 (±0.14) × 10^{-2}		NMF[d]	
$\underline{\text{G}}$GCT		4.6 (±1.6) × 10^{-3}		NMF
$\underline{\text{G}}$CGA	1.5 (±0.13) × 10^{-2}		NMF	
$\underline{\text{C}}$GCT		2.5 (±0.47) × 10^{-3}		NMF
$\underline{\text{A}}$CGA	2.1 (±0.14) × 10^{-2}		NMF	
$\underline{\text{T}}$GCT		3.8 (±1.1) × 10^{-3}		NMF
TC$\underline{\text{A}}$A	8.7 (±1.1) × 10^{-2}		9.8 (±5.2) × 10^{-3}	
AG$\underline{\text{T}}$T		1.1 (±0.1) × 10^{-1}		9.2 (±4.2) × 10^{-3}
TC$\underline{\text{T}}$A	2.2 (±0.17) × 10^{-2}		NMF	
AG$\underline{\text{A}}$T		4.4 (±1.4) × 10^{-3}		NMF
TC$\underline{\text{C}}$A	1.5 (±0.06) × 10^{-2}		NMF	
AG$\underline{\text{G}}$T		4.3 (±0.94) × 10^{-3}		NMF

[a] Experiments were performed under single-turnover conditions. See Experimental Procedures for details. Substrate concentrations were 2.5 nM. The enzyme concentration was in 200-fold excess. Reactions were initiated with 10 mM $MgCl_2$ or 2 mM $MnCl_2$. Incubations were conducted at 60 °C for a time period to achieve 10%−90% cleavage wherever it was possible. Data were based on at least three independent experiments. Standard deviations are given in parentheses. [b] The phosphorothioate substrate was the R_P isomer facing the major groove. [c] ^{7c}A: N^7-deaza-A substitution. [d] NMF: no meaningful figure.

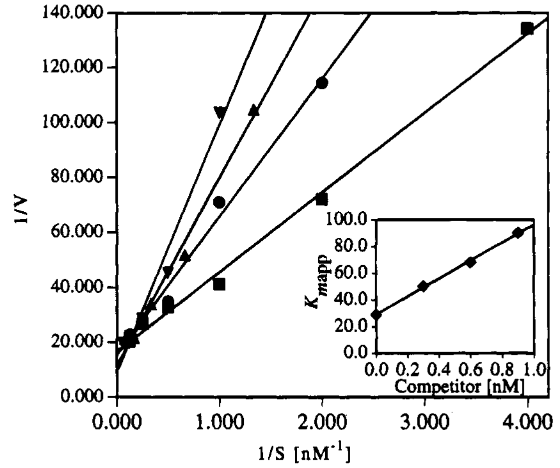

FIGURE 2: Steady state kinetics with star site (TCAA/AGTT) as competitor. Inset is a replot of apparent K_m versus competitor concentrations.

Table 3: Discrimination between Cognate and Noncognate Sites

site	K_d[a] (nM)		k_2/K_d k_3/K_d		$\Delta\Delta G^{\ddagger}$	
	Mg^{2+}	Mn^{2+}	(min nM)$^{-1}$		(kcal/mol)	
TCGA	nd[b]	nd	7.40[c]		0	
AGCT				13.20[c]		0
TsCGA	0.19	9.72	0.10		2.82	
AGCsT				0.26		2.60
TCG^{7c}A	0.07	2.36	0.74		1.52	
^{7c}AGCT				0.97		1.72
$\underline{\mathrm{C}}$CGA	nd	0.12	0.15		2.57	
$\overline{\mathrm{G}}$GCT				0.038		3.85
$\overline{\mathrm{A}}$CGA	6.14	0.10	0.21		2.35	
$\overline{\mathrm{T}}$GCT				0.38		3.86
$\overline{\mathrm{G}}$CGA	nd	0.22	0.068		3.09	
$\overline{\mathrm{C}}$GCT				0.011		4.65
$\overline{\mathrm{T}}$C$\underline{\mathrm{A}}$A	9.08	0.43	0.20		2.37	
AG$\overline{\mathrm{T}}$T				0.26		2.60
TC$\overline{\mathrm{T}}$A	nd	0.16	0.14		2.63	
AG$\overline{\mathrm{A}}$T				0.028		4.07
TC$\overline{\mathrm{C}}$A	nd	0.27	0.056		3.23	
AG$\overline{\mathrm{G}}$T				0.014		4.51
TG$\overline{\mathrm{C}}$A	18.63	207				
A$\overline{\mathrm{C}}$GT						

[a] K_d was obtained by measuring the K_i of oligonucleotides under steady state conditions. The experimental error was estimated to be 20%. See Experimental Procedures for details. [b] Not determined. [c] K_m was used to substitute K_d for cognate sequence, see text.

K_i represents their dissociation constants (K_d) (Fersht, 1985; Smith et al., 1992).

In the presence of Mg^{2+}, tight binding was achieved with the analogue-substituted oligonucleotides (Table 3), as reported previously (Zebala et al., 1992b). The N^7-deaza-A and phosphorothioate substitutions gave dissociation constants of 0.07 and 0.19 nM, respectively. These substitutions are largely isosteric; an N^7-deaza-A modification removes a putative protein−base contact, and a R_P-phosphorothioate substitutes a nonbridging oxygen with a sulfur oriented toward the major groove. As such, these changes should not severely disturb the conformation of the enzyme−substrate complex. These isosteric oligonucleotides may therefore mimic the unmodified *Taq*I−TCGA complex (Zebala et al., 1992b). In the presence of Mg^{2+}, the binding of *Taq*I to star sites was considerably weaker, exhibiting K_d values of 9 nM for the TC$\underline{\mathrm{AA}}$/AG$\underline{\mathrm{TT}}$ site and 6 nM for the $\underline{\mathrm{A}}$CGA/$\underline{\mathrm{T}}$GCT site, whereas *Taq*I bound nonspecific DNA with a K_d of 19 nM (Table 3). This demonstrates that stringent discrimination against single base-pair substitutions is achieved during the binding steps in the presence of Mg^{2+}.

In the presence of Mn^{2+}, however, analogue substitutions resulted in dissociation constants 30−50-fold higher than those observed with Mg^{2+}; the K_d was 2.36 nM for the N^7-deaza-A substitution and 9.72 nM for the phosphorothioate substitution (Table 3). In contrast, the K_d values for all the star site oligonucleotides were 1 order of magnitude *lower* than those for both analogue-substituted oligonucleotides. The star site with the highest k_{st} (TC$\underline{\mathrm{AA}}$/AG$\underline{\mathrm{TT}}$) also had the highest dissociation constant (K_d = 0.43 nM) of the six sites. The variation in the dissociation constants was no more than 4-fold between the star sites. Two simultaneous base-pair changes (T$\underline{\mathrm{GC}}$A) elevated the dissociation constant 500−2000-fold relative to the star sites. This seeming contradiction in analogue and star site dissociation constants suggests that Mn^{2+} mediates the utilization of intrinsic binding energy between enzyme and DNA in a manner fundamentally different from that of Mg^{2+}.

Energetics of Single Base-Pair Changes. Transition state interactions are best quantified by determining the energetic cost of chemical changes by comparisons of k_{st}/K_d measurements (Lesser et al., 1990) as shown in eq 1, where k_{st} is the rate constant for the chemical transformation step and K_d is the dissociation constant of ES complex. We measured the k_{st} values for the cognate site, isosterically modified sites, and star site sequences. The K_d values for these modified and star site substrates were also determined. The K_d for the cognate site could not be determined, since addition of the metal cofactor essential for specific binding results in cleavage of the substrate. Therefore the K_m value was used for the cognate site. This substitution should not affect our conclusions, for we are only comparing the relative energetic differences between two modified substrates on a qualitative basis, using the K_m value as a reference point.

The effects of sequence alteration on transition state interactions vary significantly. Substitution of 7-deaza-A for the A base, which deletes a putative protein−base contact, gave the least perturbation of transition state interactions (Table 3). In contrast, the substitution of sulfur for the nonbridging oxygen at the scissile phosphate may impose an energy barrier equivalent to a base-pair alteration. The expected higher energy cost for single base-pair changes may be viewed by their unequal impact on the two catalytic centers of the duplex DNA (Table 3). While the first base-pair changes (A-T base pair) exerted consistently more effect on the strand containing the A base alteration, the second base-pair changes (G-C base pair) showed higher costs on the strand containing the C base alteration with the exception of the preferred star site (TCAA/AGTT) (Table 3). As compared with the previously identified putative protein−base contacts (Zebala et al., 1992b), the relatively lower perturbation of transition state interactions by the preferred star site is consistent with preservation of all those contacts. None of the other star sites preserve all putative direct readout contacts.

Metal Interactions with the TaqI−DNA Complex. To determine the metal cofactor affinity for the *Taq*I−DNA complex, we measured the cleavage rate constants as a function of cofactor concentration under single-turnover conditions (See Experimental Procedures for kinetic equations). A plot of observed rate constants versus metal ion concentrations exhibited a hyperbolic curve, demonstrating saturation in the concentration range tested (Figure 3). When

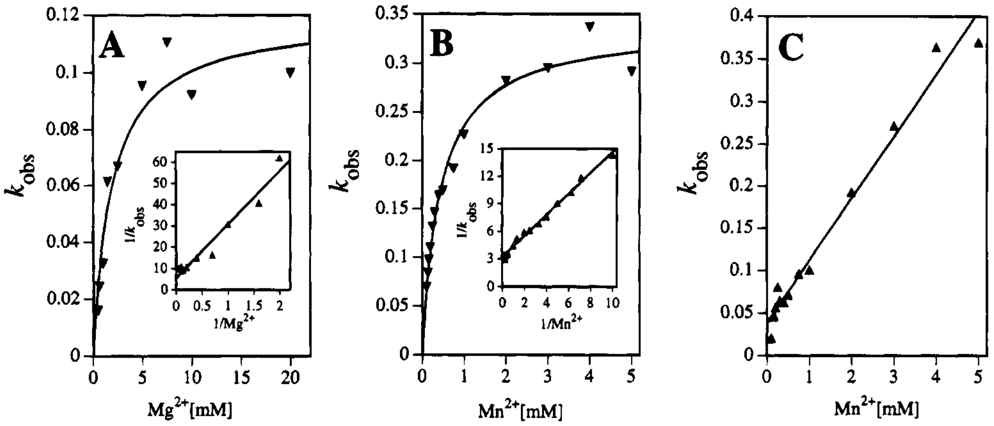

FIGURE 3: Apparent dissociation constants of metal cofactors for the *Taq*I–DNA complex. Experiments were performed under single-turnover conditions. $k_{obs} = k_2 + k_3$. Insets are corresponding reciprocal plots of original curves. Values of K_d were obtained by fitting the original curves to the Michaelis–Menten equation using the kinetics program ULTRAFIT. A. K_d of Mg^{2+} for the *Taq*I–cognate complex is 1.9 mM. B. K_d of Mn^{2+} for the *Taq*I–cognate complex is 0.39 mM. C. K_d of Mn^{2+} for the *Taq*I–star complex (TCAA/AGTT) is greater than 5 mM.

the enzyme bound the canonical TCGA site, the complex had a 5-fold higher affinity for Mn^{2+} (K_d = 0.39 mM; Figure 3B) than for Mg^{2+} (K_d = 1.9 mM; Figure 3A). When the enzyme was located on the "preferred" (TCAA/AGTT) star site, the affinity of the complex for Mn^{2+} was decreased by at least 1 order of magnitude. The absence of saturation in the range of concentrations we used indicated that this complex had a K_d far greater than 5 mM (Figure 3C). The affinity of the *Taq*I–Star complex for Mg^{2+} was not measured since cleavage was negligible even at high metal concentrations.

The higher affinity of *Taq*I–TCGA complex for Mn^{2+} was verified by a competition experiment using both metals at saturating concentrations, in which single-turnover reactions were initiated using a mixture of 10 mM Mg^{2+} and 2 mM Mn^{2+}. The "mixed metal" time course is superimposable onto that produced in the presence of Mn^{2+} alone, thereby demonstrating the higher affinity of Mn^{2+} for the metal binding site of the *Taq*I–TCGA complex (data not shown). A qualitatively similar result was obtained with *Eco*RV (Vermote & Halford, 1992).

Metal Interactions with TaqI. Given the effect Mn^{2+} has on *Taq*I specificity, we investigated the possibility of a DNA-independent metal–protein complex. We examined the events prior to formation of the specific ternary complex by varying the order of cofactor and DNA addition to the enzyme to initiate the single-turnover reaction [see also, Zebala et al. (1992a)]. Initiation of cleavage by the addition of Mg^{2+} to the *Taq*I–DNA complex yields the expected first-order reaction (Figure 4A, solid circles). This result is consistent with the hypothesis, initially proposed for *Eco*RV, that the enzyme–canonical DNA interaction organizes the metal binding site. However, a slower time course was observed when initiating the reaction by adding substrate to enzyme–Mg^{2+} (Figure 4A, open circles). This suggested that a slow step, comparable in magnitude to cleavage, precedes the formation of the specific *Taq*I–TCGA complex. Surprisingly, the results were qualitatively different for Mn^{2+} (Figure 4B). Cleavage was faster when *Taq*I was pre-equilibrated with Mn^{2+} (Figure 4B, open triangles) as compared to *Taq*I pre-equilibrated with DNA (Figure 4B, closed triangles). Specifically, cleavage was 50% complete within 2 s after starting the reaction with a preformed *Taq*I–Mn^{2+} complex. This suggests *Taq*I is activated by interaction with Mn^{2+} but not with Mg^{2+}. The implications of direct metal–protein interactions are discussed below.

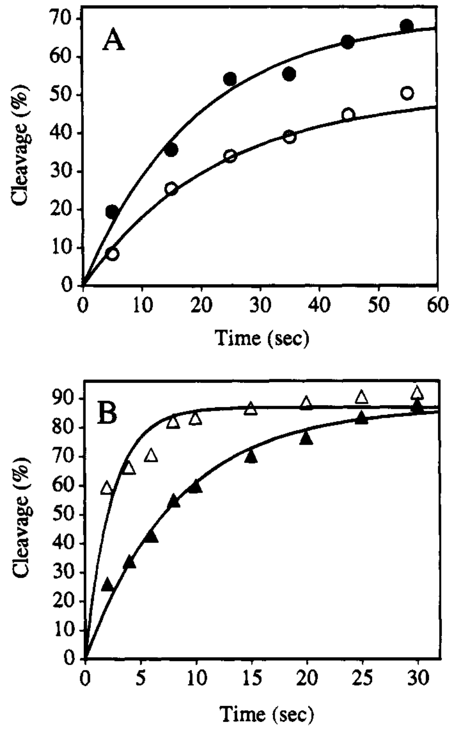

FIGURE 4: Effects of the *Taq*I–Mn^{2+} interaction on top strand cleavage (cognate site). Reactions were conducted at single-turnover conditions. A. (●) Enzyme and DNA were prebound (9 μl), and reaction was initiated with 1 μl of 100 mM $MgCl_2$; (○) enzyme and Mg^{2+} were prebound (9 μl), and reaction was initiated with 1 μl of 2.5 μM DNA. B. (▲) Enzyme and DNA were prebound (9 μl), and reaction was initiated with 1 μl of 20 mM $MnCl_2$; (△) enzyme and Mn^{2+} were prebound (9 μl), and reaction was initiated with 1 μl of 2.5 μM DNA. Bottom strand (24-mer) cleavage had the same pattern.

Steady State Kinetics. In the course of these kinetic studies, we noted that the ratio of the single-turnover to multiple-turnover rate constants was much higher for Mn^{2+} than for Mg^{2+} (Tables 1, 2, and 4). In Mg^{2+}, k_{st}/k_{cat} is 7, while in Mn^{2+} the ratio is 123, suggesting that a nonchemical step is rate limiting with Mn^{2+}. Prebinding experiments using Mn^{2+} (Figure 4B) ruled out enzyme–DNA association as the slow step, thus implicating a nonchemical step subsequent to cleavage in limiting the multiple-turnover rate.

Table 4: Steady State Constants of *Taq*I Endonuclease in Low Salt[a]

cofactor	K_m (nM)	k_{cat} (min^{-1})	k_{cat}/K_m (M^{-1} s^{-1})
Mg^{2+}	1.02 ± 0.37	0.42 ± 0.071	6.89×10^6
Mn^{2+}	1.07 ± 0.26	0.060 ± 0.0035	0.94×10^6

[a] Data were based on at least three independent experiments.

DISCUSSION

This study examines the effects of metal cofactors on the sequence specificity of *Taq*I endonuclease using both Mg^{2+} and Mn^{2+} as the cofactors. We tested the interaction of *Taq*I with cognate, isosteric analogue, star site, and nonspecific DNA sequences, measuring the effects of metal and DNA sequence on both binding and catalysis. The results provide some interesting clues as to how metal cofactors mediate sequence-specific interactions. In particular, interactions between Mn^{2+} and *Taq*I may help us to understand the role of the metal cofactor in modulating the stringency of sequence discrimination.

Metal cofactors have a profound influence on the enzymatic cycle, including ES formation, catalysis, and product release. Modulation of specificity seems to occur at an early stage of the enzymatic cycle, during formation of a *Taq*I−DNA−M^{2+} complex. With Mg^{2+}, *Taq*I endonuclease interacts with a DNA sequence in two binding modes. For a nonspecific sequence, the enzyme exhibits weak, unproductive binding (Table 3). This may imply that the nonspecific complex is incapable of forming a proper metal binding site; therefore, it impedes coordination of the metal cofactor. (The order of *Taq*I, DNA, and Mg^{2+} interactions is discussed later.) For a DNA sequence containing a cognate site, correct alignment at the protein−DNA interface leads to formation of the metal binding pocket. Subsequent coordination of Mg^{2+} cofactor assists the organization of a tight, specific complex. In view of the intrinsic binding energy utilization for transition state activation (Jencks, 1975, 1981), this *Taq*I−TCGA−Mg^{2+} complex suggests that some of the intrinsic binding energy is used for transition state activation but that a large amount of the energy is realized at the ES level resulting in tight binding. In the case of a single base-pair substitution, substrate affinity is drastically diminished, such that dissociation constants approximate that of nonspecific DNA (Table 3). We suggest that in these cases lack of proper alignment at the interface in the star site sequences precludes formation of an activated ES complex which, in turn, results in a disorganized catalytic center and the attendant failure to coordinate Mg^{2+}. This view is supported by the observation that the affinity of *Taq*I for its cognate sequence is positively influenced by the presence of cofactor (Zebala et al., 1992a) as shown previously with *Eco*RV (Thielking et al., 1992; Vermote & Halford, 1992) and is consistent with the "allosteric activation" model proposed for *Eco*RI (McClarin et al., 1986; Wright et al., 1989).

Unlike the binding mode in the presence of Mg^{2+}, Mn^{2+} is able to distinguish DNA sequences in three ways. For an isosterically modified cognate sequence, the apparent weak binding correlates to a faster single-turnover rate with Mn^{2+} than Mg^{2+} (Tables 1−3). Applying the intrinsic binding energy concept, Mn^{2+} seems to be conferring the intrinsic binding energy to activating the *Taq*I−TCGA complex for transition state interactions. As such, the *Taq*I−cognate−Mn^{2+} complex becomes highly activated. The tight binding to a star site sequence could be explained by the high affinity of Mn^{2+} for a *Taq*I−DNA complex (Figure 3), which facilitates the retention of the metal cofactor in the complex. On the other hand, the higher affinity of *Taq*I for its star sites may reflect limited use of intrinsic binding energy for energetically costly ES activation in comparison with its cognate site. In doing so, Mn^{2+} may compensate for lower surface complementarity in the star site complex. As noted with Mg^{2+}, changing two base pairs in a cognate sequence would severely disturb the *Taq*I−DNA interface and thus prevent formation of a specific, activated *Taq*I−DNA−Mn^{2+} complex.

Scheme 2

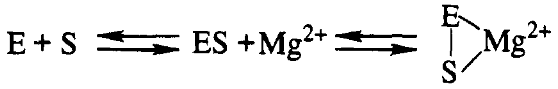

Scheme 3

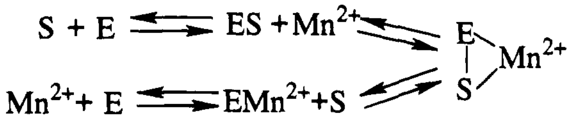

To elucidate how Mn^{2+} modulates the enzymatic cycle and relaxes specificity, we have investigated the role of Mn^{2+}−*Taq*I interactions on the single-turnover rate (Figure 4). The results suggest that, surprisingly, Mn^{2+} may interact with *Taq*I in a DNA-independent fashion. By initiating and stabilizing an active conformation of the enzyme, Mn^{2+} imparts additional leverage for ES activation and transition state interactions. As a result, the *Taq*I−TCGA−Mn^{2+} complex attains a higher level of activation than the *Taq*I−TCGA−Mg^{2+} complex and shows faster single-turnover rates (Tables 1 and 2). This mode of action may underlie the relaxation of sequence specificity as well. The Mn^{2+}-mediated activation may accommodate star site cleavage in two ways. First, the activated Mn^{2+}−*Taq*I complex enhances activation of the ternary *Taq*I−star−Mn^{2+} complex. Second, the intrinsic affinity of Mn^{2+} for the enzyme facilitates the retention of Mn^{2+} molecule at the catalytic center of the partially activated *Taq*I−star−Mn^{2+} complex. In support of this view, several amino acid residues thought to be involved in binding and/or catalysis have been identified by metal (Mn^{2+} and Fe^{2+})-mediated affinity cleavage of *Taq*I protein (W. Cao and F. Barany, unpublished).

Kinetic analysis of *Eco*RV endonuclease suggests that formation of the E−S−Mg^{2+} ternary complex is ordered as depicted in Scheme 2, i.e., the binding of enzyme to substrate creates a binding site for the cofactor (Taylor & Halford, 1989). Indeed, the crystal structure suggests that cognate DNA binding brings the scissile phosphate to the vicinity of the active site, where the oxygens of the scissile phosphate and two aspartate side chains (D74 and D90) provide putative ligands for metal coordination (Winkler et al., 1991, 1993). Varying the order of Mg^{2+} and DNA addition to *Taq*I to initiate the single-turnover reaction is consistent with a similar ordered pathway using this metal cofactor (Figure 4A).

Ordered addition single-turnover experiments with Mn^{2+} suggest a different pathway for formation of the *Taq*I−DNA−Mn^{2+} ternary complex (Figure 4B) as shown in Scheme 3. Two models may account for Mn^{2+} activation of the ternary complex. (i) One Mn^{2+} binds to the catalytic site. Mn^{2+} may readily coordinate with ligands provided by the enzyme, creating a substrate binding site and allowing for rapid activation of the substrate. (ii) Two (or more than two) Mn^{2+} ions may be involved; one binds a regulatory site to activate the enzyme, and the other plays a catalytic role, as has been proposed for pyruvate kinase (Villafranca, 1974) and DNA polymerase (Ferrin et al., 1986). A "two-metal" mechanism was proposed for 3′−5′ exonuclease of *Escherichia coli* DNA polymerase (Beese & Steitz, 1991), DNA polymerase I (Derbyshire et al., 1988), and *Eco*RV endonuclease [Winkler et al. (1993); S. Halford, personal communication]. We currently have no experimental evidence to rule out models involving one or more than one metal ions in binding and catalysis.

Finally, Mg^{2+} and Mn^{2+} cofactors display different steady state kinetics. While k_{st} values are higher with Mn^{2+} (Tables 1 and 2), the k_{cat} value is 7-fold lower than with Mg^{2+} (Table 4). In addition, an initial burst phase was observed during initial steady state rate measurements when using Mn^{2+} but not Mg^{2+} as a cofactor (W. Cao and F. Barany, unpublished). This result suggests a rate-limiting step subsequent to catalysis dominates k_{cat} when Mn^{2+} is the cofactor. This slow step may be the dissociation of Mn^{2+} from the cleaved *Taq*I−TCGA−Mn^{2+} complex. Upon Mn^{2+} dissociation, the *Taq*I−product complex rapidly disassembles (suggested by F. Winkler, personal communication).

CONCLUSION

We have investigated the kinetic behavior of *Taq*I endonuclease using either Mg^{2+} or Mn^{2+} as the metal cofactors, focusing on the mechanism of substrate specificity. Consistent with our previous studies, data from the present study point to mechanistic similarities between *Taq*I and *Eco*RV, as these two restriction endonucleases both require a metal cofactor for specific binding. By comparing the effects on binding and catalysis, this study reveals the differential binding modes of *Taq*I with regard to the metal cofactors. While *Taq*I−TCGA−Mg^{2+} complex attains tight and specific binding, *Taq*I−TCGA−Mn^{2+} complex represents a highly activated specific form poised for transition state interactions. Furthermore, this study provides kinetic evidence for a direct Mn^{2+}−*Taq*I interaction, which may underlie the marked differences observed in the enzymatic cycle between Mg^{2+} and Mn^{2+}. Many important questions, however, remain to be answered. For example, what is the structural basis of this interaction? How many Mn^{2+} ions are involved in binding, activation, and catalysis? Further characterization of the interactions between Mn^{2+} and the enzyme using both biophysical and biochemical means may prove to be fruitful for fully defining the molecular basis of the substrate specificity of the *Taq*I endonuclease, as well as other enzymes.

ACKNOWLEDGMENT

The authors gratefully acknowledge Fritz Winkler, Steven Halford, Linda Jen-Jacobson, Richard Gumport, Bernard Connolly, Manfred Kroger, Joe Heitman, Aneel Aggarwal, David Cowburn, Geoffrey Wilson, Hamilton Smith, and Richard Roberts for thoughtful discussions. We also thank Jianying Luo, Darren Day, John Zebala, Antje Koller, Shengwen Li, and Kenan Onel for their help, discussion, and assistance.

REFERENCES

Aiken, C. R., Fisher, E. W., & Gumport, R. I. (1991) *J. Biol. Chem. 266*, 19063−19069.

Applied Biosystems Inc. (1992) *The complete guide—evaluating and isolating synthetic oligonucleotides*, Applied Biosystems Inc., Foster City, CA.

Barany, F. (1988a) *Gene 65*, 149−165.

Barany, F. (1988b) *Gene 65*, 167−177.

Beese, L. D. S., & Steitz, T. A. (1991) *EMBO J. 10*, 25−33.

Derbyshire, V., Freemont, P. S., Sanderson, M. R., Beese, L., Friedman, J. M., Joyce, C. M., & Steitz, T. A. (1988) *Science 240*, 199−201.

Ferrin, L. J., Beckman, R. A., Loeb, L. A., & Mildvan, A. S. (1986) in *Manganese in metabolism and enzyme function* (Schramm, V. L., & Wedler, F. C., Eds.) pp 259−273, Academic Press, Inc., Orlando, FL.

Fersht, A. (1985) *Enzyme structure and mechanism*, 2nd ed., W. H. Freeman and Co., New York.

Halford, S. E., Lovelady, B. M., & McCallum, S. A. (1986) *Gene 41*, 173−181.

Halford, S. E., Taylor, J. D., Vermote, C. L. M., & Vipond, I. B. (1993) *Nucleic Acids Mol. Biol. 7*, 47−69.

Heitman, J. (1993) in *Genetic Engineering, Principles and Methods* (Setlow, J., Ed.) pp 57−108, Plenum Press, New York.

Jencks, W. P. (1975) *Adv. Enzymol. 43*, 219−410.

Jencks, W. P. (1981) *Proc. Natl. Acad. Sci. U.S.A. 78*, 4046−4050.

Lesser, D. R., Kurpiewski, M. R., & Jen-Jacobson, L. (1990) *Science 250*, 776−786.

Lesser, D. R., Kurpiewski, M. R., Waters, T., Connolly, B. A., & Jen-Jacobson, L. (1993) *Proc. Natl. Acad. Sci. U. S. A. 90*, 7548−7552.

Mayer, A. N., & Barany, F. (1994) *J. Biol. Chem. 269*, 29067−29076.

McClarin, J. A., Frederick, C. A., Wang, B. C., Greene, P. J., Boyer, H. W., Grable, J., & Rosenberg, J. M. (1986) *Science 234*, 1526−1541.

Polisky, B., Greene, P., Garfin, D. E., McCarthy, B. J., Goodman, H. M., & Boyer, H. W. (1975) *Proc. Natl. Acad. Sci. U.S.A. 72*, 3310−3314.

Roberts, R. J., & Halford, S. E. (1993) in *Nucleases* (Linn, S. M., & Roberts, R. J., Eds.) pp 35−88, Cold Spring Harbor Laboratory Press, Cold Spring Harbor, NY.

Rosenberg, J. M. (1991) *Curr. Opin. Struct. Biol. 1*, 104−113.

Segel, I. H. (1975) *Enzyme kinetics—Behavior and Analysis of Rapid Equilibrium and Steady-State Enzyme Systems*, John Wiley & Sons, New York.

Smith, D., Burgin, A. B., Haas, E. S., & Pace, N. R. (1992) *J. Biol. Chem. 267*, 2429−2436.

Smith, H. O. (1979) *Science 205*, 455−462.

Taylor, J. D., & Halford, S. E. (1989) *Biochemistry 28*, 6198−6207.

Taylor, J. D., & Halford, S. E. (1992) *Biochemistry 31*, 90−97.

Taylor, J. D., Goodall, A. J., Vermote, C. L., & Halford, S. E. (1990) *Biochemistry 29*, 10727−10733.

Taylor, J. D., Badcoe, I. G., Clarke, A. R., & Halford, S. E. (1991) *Biochemistry 30*, 8743−8753.

Thielking, V., Selent, U., Köhler, E., Landgraf, A., Wolfes, H., Alves, J., & Pingoud, A. (1992) *Biochemistry 31*, 3727−3732.

United States Biochemical. (1992) *Molecular Biology Reagents/Protocols*, United States Biochemical Corp., Cleveland, OH.

Vermote, C. L. M., & Halford, S. E. (1992) *Biochemistry 31*, 6082−6089.

Vermote, C. L. M., Vipond, B., & Halford, S. E. (1992) *Biochemistry 31*, 6089−6097.

Villafranca, J. J. (1974) in *Metal ions in biological systems, Vol. 4, metal ions as probes* (Sigel, H., Ed.) pp 29−59, Marcel Dekker, Inc., New York.

Winkler, F. K., D'Arcy, A., Blocker, H., Frank, R., & van Boom, J. H. (1991) *J. Mol. Biol. 217*, 235−238.

Winkler, F. K., Banner, D. W., Oefner, C., Tsernoglou, D., Brown, R. S., Heathman, S. P., Bryan, R. K., Martin, P. D., Petratos, K., & Wilson, K. S. (1993) *EMBO J. 12*, 1781−1795.

Wright, D. J., King, K., & Modrich, P. (1989) *J. Biol. Chem. 264*, 11816−11821.

Zebala, J., Choi, J., & Barany, F. (1992a) *J. Biol. Chem. 267*, 8097−8105.

Zebala, J. A., Choi, J., Trainor, G. L., & Barany, F. (1992b) *J. Biol. Chem. 267*, 8106−8116.

BI942327G